Cytokine signalling by grafted neuroectodermal stem cells rescues motoneurons destined to die

Krisztián Pajer[1], Georg Feichtinger[2], Gábor Márton[1], Sonja Sabitzer[3], Dieter Klein[3], Heinz Redl[2], Antal Nógrádi[1,2]*

[1]Department of Anatomy, Histology and Embryology, Faculty of Medicine, University of Szeged, Szeged, Hungary; [2]Ludwig Boltzmann Institute for Experimental and Clinical Traumatology, Vienna, Austria; [3]VetCORE Technology Centre for Research at the University of Veterinary Medicine in Vienna, Austria

*corresponding author:
Antal Nógrádi
Dept. of Anatomy, Histology and Embryology, Faculty of Medicine, University of Szeged
H-6724 Szeged, Kossuth L. sgt. 40.
Tel.: +36-62-545786
Fax: +36-62-546118

Running title: Cytokine signalling rescues motoneurons

Number of pages: 32

Number of figures: 7

Number of words for Abstract: 199

Number of words for Introduction: 414

Number of words for Discussion: 683

Conflict of Interest: The authors declare no competing financial interests

Acknowledgements

The excellent technical help of E. Katona and E. Kovács is gratefully acknowledged. The authors are indebted to David Durham for a critical reading of the manuscript. KP was a recipient of a Marie Curie Short-term Fellowship. We thank the Lorenz Böhler Fond, Austria, for its generous support.

Abstract

Following an injury to their axons close to the cell body, adult motoneurons generally die. This type of injury, typically caused by avulsion of the spinal ventral root, initiates the activation of astrocytes and microglial cells and the extracellular space becomes loaded with excessive amounts of excitotoxic glutamate. We have provided evidence that, following ventral root avulsion and reimplantation, murine embryonic neuroectodermal stem cells (NE-GFP-4C) grafted into the rat spinal cord rescue the vast majority of the motoneurons that would otherwise die, and enable them to reinnervate peripheral targets. Stem cell grafts produced the modulatory cytokines IL-1-alpha, IL-6, IL-10, TNF-alpha and MIP-1-alpha, but not neurotrophic factors. The neurons and astrocytes in the ventral horn of grafted animals also produced IL-6 and MIP-1-alpha, indicating a strong interaction between the graft and the host tissue. The infusion of function-blocking antibodies against all cytokines into the grafted cords completely abolished their motoneuron-rescuing effect, while neutralization of only IL-10 suggested its strong effectivity as concerns motoneuron survival and a milder effect on reinnervation.

It is suggested that, apart from the anti-inflammatory function of IL-10, the pro-inflammatory cytokines produced exert a strong modulatory function in the CNS, promoting the prevention of neuronal cell death.

Key words

avulsion injury, motoneuron death, reinnervation, neuronal survival

Introduction

If their axons are injured relatively distant from the cell body, adult motoneurons usually survive. However, axonal injuries close to the cell body, such as root avulsion injuries, induce the death of the vast majority of the affected motoneurons (Koliatsos et al, 1994; Nógrádi et al, 2007). The injured motoneurons become vulnerable to the excessive amounts of glutamate delivered into the extracellular space from the nerve terminals, initiated by nitric oxide(McNaught and Brown, 1998): glutamate activates N-methyl-D-aspartate (NMDA) receptors (Tikka and Koistinaho, 2001), which in turn induce an excessive influx of calcium into the damaged cells (Hahn et al, 1988). The glutamate excitotoxicity is further augmented by the microglial reactivity around the injured motoneurons (Penas et al, 2009), eventually leading to cell death (Brown and Neher, 2010; Giulian et al, 1993; Regan and Choi, 1991).

Potent molecules that antagonize the effects of glutamate toxicity are known to be able to rescue around 70% of the injured motoneurons, provided that the treatment is applied within 10-12 days after the occurence of the injury (Nógrádi et al, 2007; Nógrádi and Vrbová, 2001; Pintér et al, 2010). Other treatment strategies involving for example neurotrophins, particularly GDNF and BDNF produced by grafted stem cells or applied directly to the injured cord, also prevent motoneuron death (Blits et al, 2004; Eggers et al, 2008; Hell et al, 2009; Su et al, 2009), although neurotrophins typically do not promote axonal regeneration, but rather sprouting at the site of application. On the other hand, it is generally accepted that neural progenitor or stem cells shown to produce neurotrophic factors *in vitro* are effective to promote survival of injured motoneurons (Blits et al, 2004; Hell et al, 2009; Su et al, 2009). However, other potential mechanisms to rescue damaged motoneurons by changing the microenvironment of these cells are not explored. To address this question, we investigated whether a well established clonal neuroectodermal stem cell line, known to promote regeneration in the lesioned brain (Demeter et al, 2004, Zádori et al, 2011) is able to prevent motoneuron death after avulsion injury, and if so what factors are responsible for the motoneuron-rescuing effect. We here report a remarkable capacity of neuroectodermal stem

cells to promote the survival and regeneration of injured motoneurons otherwise destined to die by secreting a set of cytokines. Moreover, it is shown that stem cell grafts interact with the host environment and induce a pattern of cytokine expression by host neurons and astrocytes similar to that of grafted stem cells.

Materials and methods

Maintenance of NE-GFP-4C stem cells

The clonal neuroectodermal stem cells (NE-GFP-4C cells, a gift from Dr. E. Madarász, Institute of Experimental Medicine, Hungarian Academy of Sciences; also available from ATCC, No. CRL-2926) were originally isolated from 9-day-old forebrain vesicles of embryos of transgenic mice lacking tumour suppressor gene p53, and were made to produce eGFP as described previously (Schlett and Madarasz, 1997) . NE-GFP-4C stem cells were maintained on nuncloned petri dishes (VWR International, Debrecen, Hungary) in High-glucose Dulbecco Modified Essential Medium (H-DMEM, Sigma, Hungary) supplemented with 10% foetal calf serum (Invitrogen/life Technologies, Paisley, UK) at 37 °C and 5% CO_2. Floating cells appeared after 3 days and cultures were passaged every 2 days. All cell cultures underwent at least two, but no more than five passages before transplantation.

Ventral root avulsion-reimplantation and transplantation of NE-GFP-4C stem cells

A total of 136 Sprague-Dawley rats (Biological Services, University of Szeged, 180-220 g body weight) were used. Ninety-three animals received stem cell grafts and 36 were used as operated controls (avulsion and reimplantation only). Seventy animals participated in retrograde labelling and immunohistochemistry, 48 operated and 9 intact animals in semiquantitative and qPCR studies, 8 animals in tension recording studies, and 15 animals in functional blocking experiments.

All the operations were carried out under deep ketamine-xylazine anaesthesia (ketamine hydrochloride, 110 mg/kg body weight; xylazine [Rompun] 12 mg/kg body weight) and sterile precautions. Laminectomy was performed at the level of T13–L1, the dura was opened and the left L4 ventral root was pulled out, leaving the dorsal roots intact. The free end of the ventral root was then inserted into the ventrolateral part of segment L4 and $5x10^4$, 1x, 2x or $3x10^5$ stem cells were injected into the segment at the site of grafting. The spinal cord was covered with the remaining

dura, the wound was closed and the animals were allowed to recover (Nógrádi and Vrbová, 1996, 2001). The control experiments involved either intact animals or rats whose L4 root was avulsed and reimplanted without a stem cell graft. Animals survived for 2, 5, 10, 14 or 16 days or for 1, 3 or 6 months. No immunosupressive treatment was applied. The experiments were carried out with the approval of the Committee for Animal Experiments at the University of Szeged regarding the care and use of animals for experimental procedures. All the procedures were carried out in full accordance with the Helsinki Declaration on Animal Rights. Adequate care was taken to minimize pain and discomfort.

Retrograde labelling

Three months after the surgery, the 5 animals per group were deeply anaesthetized as described above. On the operated side, the ventral ramus of the left L4 spinal nerve was sectioned and the proximal stump of the nerve was covered with a few Fast Blue crystals. Four days after the application of this fluorescent dye, the animals were reanaesthetized and were perfused transcardially with 4% paraformaldehyde in 0.1 mol/l phosphate buffer (pH=7.4).

Semiquantitative PCR, list of factors

Spinal cords were homogenized twice for 10 sec in 600 µl RLT buffer + ß-MeETOH (Qiagen GmbH, Hilden, Germany) with a MagNaLyser (Roche, Rotkreuz, Switzerland) at a speed of 5,500 rpm with an intermediate pause for 5 min on ice. The resulting lysates were incubated on ice and subjected to centrifugation at 13,000 rpm for 1 min at room temperature. The lysates were subsequently used for RNA extraction with the QIAcube robot system (Qiagen) and the RNeasy Mini Kit protocol for large samples (Qiagen). After DNaseI treatment (Turbo DNA-free Kit, Ambion, Austin, TX, USA), the RNA was measured both qualitatively and quantitatively with an Agilent 2100 Bioanalyzer (Agilent, Vienna, Austria). An RNA Lab chip (Agilent RNA 6000 Nano Reagents) was used to determine the RNA integrity number. cDNA was synthetized with a

High-Capacity Reverse Transcription Kit (Applied Biosystems, Foster City, CA, USA) The appropriate 5' and 3 ' primers for PCR were designed manually and then tested with AmplifX software. The appropriate conditions (e.g. annealing temperatures) for each cytokine, chemokine and neurotrophic factor were first established by gradient-PCR, using a positive control consisting of mouse and rat embryo tissue or injured mouse and rat spinal cord. To establish the quantification in the linear range, different cycle numbers were used depending on the target genes: IL-1-alpha, IL-1-beta, TGF-beta, MIP-1-alpha and PDGF-alpha were amplified at 30 cycles, while hypoxanthine-guanine phosphoribosyltransferase (HPRT), the other cytokines (IL-6, IL-10, MCP-1, MCSF and TNF-alpha) and the neurotrophic factors (BDNF, GDNF, NT-3, NT-4/5, PDGF-beta, and PTN) were amplified at 35 cycles. The RT-PCR results for the cytokines, chemokines and neurotrophic factors at each time point (2, 5, 10 and 14 days after surgery) were expressed as a proportion of the corresponding intensity value of the HPRT product (densitometric measurement).

Laser capture microdissection (LCM), quality control of RNA

All tissues were quick-frozen in liquid nitrogen and stored at -80 °C until further use. LCM was performed with the Veritas instrument (Arcturus, CA, USA), equipped with a cutting laser (349 nm) to cut a narrower outline around the region of interest and a capture laser (810 nm) to capture the entire region within the outline. The procedure has been described previously (Jais et al, 2011). In brief, 10 µm thick tissue sections were cut on a Leica CryoCut Jung CM1800 cryostat (Leica Instruments, Nußloch, Germany) by using an RNAse-free technique, mounted onto special membrane slides (Molecular Machines & Industries, Glattbrugg, Switzerland) and stained immediately after cutting with the HistoGene LCM Frozen Section Staining kit (MDS Analytical Technologies, Ismaning, Germany). The sections were then cleared in xylene for 5 min and either used directly for microdissection or stored at -80 °C until further use. Regions of interest were cut and captured into CapSure Macro LCM caps (MDS, Ismaning, Germany). The laser power setting ranged from 60 to 80 mW, and the pulse settings from 1,700 to 2,500 µsec. Spot size was

determined prior to microdissection and adapted to each tissue type. During an LCM session, dissection of an area of approximately 200,000 – 250,000 µm² (~ 1,000 cells) led to amplifiable results in the subsequent qPCR. The remaining tissue on the slide was used for RNA quality measurement using the RNeasy Micro Kit (Qiagen) for RNA isolation. The protocol including the DNaseI treatment was carried out directly on the columns. After the overall procedures, the RNA quality measurements were analysed with the Agilent 2100 Bioanalyzer applying the RNA 6000 pico Lab chip (Agilent).

Design of primers used for quantitative RT-PCR studies

The primers of the assays used in this study were designed through the use of the Primer Express software version 2.0 (Applied Biosystems). The house-keeping gene assays were designed to detect mouse and rat mRNA transcripts and were based on mRNA alignments (SECentral software, Cary, NC, USA) using the following reference genes: mouse BC082592 and rat X02231 sequences for GAPDH, and mouse NM_013556 and rat BC098629 for the HPRT assay. In order to exclude the detection of DNA, the primers were located on different exons. The primers used for the GAPDH assay were: sense: 5'- GGC CTT CCG TGT TCC TAC C -3´ and antisense: 5'- GCC TGC TTC ACC ACC TTC TT - 3´; and for HPRT: sense: 5'- GGT GGA GAT GAT CTC TCA ACT TTA AC -3´ and antisense: 5'- TGT ATC CAA CAC TTC GAG AGG TCC -3´.

The genes of interest were designed to detect mouse and rat sequences, too. The primers used for the different assays were: MIP: sense: 5'- TGC CCT TGC TGT TCT TCT C - 3' and antisense: 5'- ATT CTT GGA CCC AGG TCT CTT - 3'; PDGF: sense: 5' – TAG ACT CCG TAG GGG CTG A – 5' and antisense: CAA TAC TTC TCT TCC TGC GAA TGG - 5'; TNFa: sense: 3'- ACT GAA CTT CGG GGT GAT CG - 5' and antisense: 5'- TTG AAG AGA ACC TGG GAG TAG A -3'; IL-1: sense: 5'- AGA CCA TCC AAC CCA GAT CA - 3' and antisense: 5'- CGG TCT CAC TAC CTG TGA TG -3'; IL10: sense: 5'- ATG GCC CAG AAA TCA AGG-3' and antisense: 5'- CGA GGT TTT CCA AGG AGT TG -3'; IL6: sense: TTC CCT ACT TCA CAA GTC CGG-3' and antisense:

5’- TAC AAT CAG AAT TGC CAT TGC A-3’; PDGFnew: sense: 5’- CTG GCT CGA AGT CAG ATC CAC -3’ and antisense: 5’- GGG CTC TCA GAC TTG TCT CCA -3’.

All assays were validated by using standard dilution series of a positive control over at least 4 log decades. The reaction efficiency was calculated from each standard curve via the formula: E: $10^{-1/slope}$ -1.

Quantitative RT-PCR (qRT-PCR)

A two-step qRT-PCR was performed with the High-Capacity Reverse Transcription Kit (Applied Biosystems) for cDNA synthesis and adjacent qPCR measurements were performed with the Power Sybr Green Kit (Applied Biosystems). The cDNA was synthetized on a StepOnePlus cycler (Applied Biosystems) and the qPCR was performed on the 7900HT Sequence Detection System (Applied Biosystems). The expression levels of different genes of interest (MIP-1-alpha, TNF-alpha, IL-1-alpha, IL-6 and IL-10) were measured by qRT-PCR (Klein, 2002). The relative expression levels of these genes were calculated in relation to two different house-keeping genes (glyceraldehyde-3-phosphate-dehydrogenase [GAPDH] and HPRT) using the ddCt method. As the data obtained with the use of GAPDH appeared to be more reliable, these are presented here.

Immunohistochemistry

For spinal cords 25 µm transverse sections were cut on a cryostat (Leica CM 1850, Leica GmbH, Nussloch, Germany) and mounted onto gelatin-coated glass slides. Non-specific binding sites were subsequently blocked with 3% normal donkey, goat or horse serum. Primary antibodies were incubated overnight at 4 °C, washed, and then incubated with fluorescent-conjugated secondary antibodies for 1 h at room temperature. The following primary antibodies were used: anti-mouse IL-1-alpha **(R&D Systems Cat# AF-400-NA RRID:AB_354473)**, IL-6 **(R&D Systems Cat# AF-406-NA RRID:AB_354478)**, TNF-alpha **(R&D Systems Cat# AF-410-NA RRID:AB_354479)**, MIP-1 alpha **(R&D Systems Cat# AF-450-NA RRID:AB_354492)** (1:50, all

from R&D Systems, Minneapolis, MN, USA), anti-mouse IL-10 **(BioLegend Cat# 505011 RRID:AB_389223**), (1:400, Biolegend, San Diego, CA, USA), mouse anti-GFAP **(Santa Cruz Biotechnology, Inc. Cat# sc-71141 RRID:AB_1124625)** (1:100 Santa Cruz Biotechnology, Inc, CA, USA), polyclonal chicken anti-green fluorescent protein (GFP) **(EMD Millipore Cat# AB16901 RRID:AB_90890)** (1:2,000 Chemicon), biotinylated Griffonia (Bandeira) simplicifolia lectin B_4 **(**(GSA-B_4, 1:200, Vector Labs, Burlingame, CA, USA), anti-mouse/rat IL-1-alpha **(Abbiotec Cat# 250715 RRID:AB_2124091),** IL-6 **(Abbiotec Cat# 250717 RRID:AB_2127453)**, IL-10 **(Abbiotec Cat# 250713 RRID:AB_2125107)**, TNF-alpha **(Abbiotec Cat# 250844 RRID:AB_2204102)** and MIP-1-alpha **(Abbiotec Cat# 251416 RRID:AB_10637571)** (1:200, all from Abbiotec, San Diego, CA, USA), goat anti-choline acetyltransferase **(Merck Cat# AB144P RRID:AB_11214092)** (1:200, Millipore, Billerica, MA, USA), anti-mouse M6 (mouse-specific neuron marker, 1:400 DSHB, IA, USA), anti-mouse M2 (mouse-specific astrocyte marker, 1:400, DSHB), anti-mouse MOG **(R&D Systems Cat# MAB2439 RRID:AB_2145548)** (mouse-specific oligodendrocyte marker, 1:50, R&D Systems, Minneapolis, MN) and anti-SSEA-1 (stage-specific mouse embryonic antigen-1, 1:400, DSHB). Secondary antibodies were used as follows: Alexa Fluor 594 donkey anti-rat **(Life Technologies Cat# A21209 RRID:AB_10562899)**, Alexa Fluor 546 goat anti-rabbit **(Life Technologies Cat# A10040 RRID:AB_11181145)**, Alexa Fluor 546 donkey anti-goat **(Life Technologies Cat# A11056 RRID:AB_10584485)**, Alexa Fluor 488 goat anti-chicken **(Life Technologies Cat# A11039 RRID:AB_10563770)**, horse biotinylated anti-goat IgG (H+L) (and horse biotinylated anti-mouse IgG (H+L). Immunohistochemistry and lectin histochemistry were also visualized with either the streptavidin Alexa Fluor 546 conjugate or the streptavidin Alexa Fluor 488 conjugate (1:400, Invitrogen). To validate TNF-alpha and IL-1-alpha immunohistochemistry, Mg^3HeLa cells transfected with TNF-alpha plasmid (a kind gift from Ernő Duda, at the Biological Research Centre, Szeged, Hungary) and rat testis were used, respectively. Fluorescence signals were detected in an Olympus BX50 epifluorescence microscope equipped with a DP70 digital camera (Olympus Ltd, Tokyo, Japan). Confocal microscopic images were

obtained by using an Olympus FluoView® FV10i compact confocal microscope.

Function-blocking antibody experiments

Adult female rats (n=5 in each set of experiments) were deeply anaesthetized and the avulsion-reimplantation of the L4 ventral root and transplantation of $3x10^5$ NE-GFP-4C cells were performed as described above. A mini-osmotic pump (Alzet Osmotic Pumps, Cupertino, CA, USA; type 1002, 100 µl volume) filled with a mixture of function-blocking antibodies against IL-1a **(R&D Systems Cat# AF-400-NA RRID:AB_354473)**, IL-6 **(R&D Systems Cat# AF-406-NA RRID:AB_354478)**, TNF-alpha **(R&D Systems Cat# AF-410-NA RRID:AB_354479)**, MIP-1 alpha **(R&D Systems Cat# AF-450-NA RRID:AB_354492)** (4 µg/ml working concentration, all from R&D Systems, Minneapolis, MN, USA) and IL-10 **(BioLegend Cat# 505011 RRID:AB_389223**) (Biolegend, San Diego, CA, USA) was placed subcutaneously in the dorsal region (ARG + 5 factors neutralization). All antibodies were specific to mouse epitopes only. A silicone tube (Degania Silicone Ltd, Kibbutz Degania, Israel, 0.3 mm in internal diameter) extended from the mini-pump to the spinal cord and its distal end was inserted into the cord at the site of grafting. The tube was fixed to the surrounding musculature with 8-0 sutures (Ethilon) to avoid moving in or out of the spinal cord. In another set of experiments osmotic pumps filled with IL-10 antibody only (4 µg/ml working concentration, ARG + IL-10 neutralization) were used. Control animals received pumps filled with identical volumes of antibody-specific IgG isotypes only (ARG+IgG; polyclonal goat IgG **(R&D Systems Cat# AB-108-C RRID:AB_354267)** for the replacement of MIP-1a, IL-1a, IL-6 and TNF-alpha antibodies and monoclonal rat IgG2A **(R&D Systems Cat# MAB006 RRID:AB_357349)** for the replacement of IL-10 antibody, 4 µg/ml working concentration, all from R&D Systems, Minneapolis, MN, USA). The pumps were removed 2 weeks after the operation. The animals survived for 3 months and were then processed for motoneuron counts and histological analyses.

Cell counts

The number of retrogradely labelled cells were determined on 25 μm thick serial cryostat sections. To avoid double counting of neurons present in consecutive sections, the retrogradely labelled neurons were mapped with the aid of an Olympus (Olympus Ltd, Tokyo, Japan) drawing tube, and their locations were compared with those of the labelled neurons in the previous section (Nógrádi et al, 2007; Pintér et al, 2010). All sections from the L4 motoneuron pool were used.

Quantification of astrocyte and microglia/macrophage density

To assess the density of GFAP-positive astrocytes and GSA-B4-positive microglia/macrophages in injured and grafted ventral horns, we photographed injured, grafted and contralateral intact horns for each rat at a 10-fold primary magnification, using a Olympus BX50 epifluorescence microscope at a distance of 0.5, 1, 1.5, and 2 mm rostral and caudal to the reimplanted ventral root (n=5/group). The macrophage marker GSA-B4 isolectin was used as this lectin is able to bind to both microglial cells of the spinal cord and invading macrophages. With ImageJ Software **(ImageJ, RRID:nif-0000-30467**), we measured the relative densities of GFAP and GSA-B4 immunoreactivity in the ventral horns. The background/autofluorescence of unstained samples as reference intensity was then subtracted from the intensity of injured grafted and of intact ventral horns in order to determine the final density. The GFAP and GSA-B4 intensity of the injured and grafted ventral horns was then divided by that of the contralateral intact ventral horns. As GSA-B4 labels the endothelial cells of some capillaries, the density of the capillaries was deducted from the total densities. We additionally performed automatic thresholding for each image by using NIH ImageJ software to determine the threshold for the specific signal. After the threshold had been set, the density above the threshold was quantified.

Analysis of locomotion pattern – CatWalk gait analysis

For determination and analysis of the parameters of the hindlimb movement pattern, the 'CatWalk'

automated quantitative gait analysis system (Noldus Ltd, Wageningen, The Netherlands) was used at the end of the 3 months survival period. This computer-assisted method of locomotor analysis made it possible to quantify several gait parameters, including the duration and speed of different phases of the step cycle and print areas detected during locomotion. The following parameters were taken into account during the analysis: *the print area*: the total floor area contacted by the paw during the stance phase;

the maximum print area: the area contacted by the paw at the moment of maximum paw-floor contact during the stance phase;

the box length and width: the parameters describing the length and width of the print area;

the stride length: the distance between two consecutive paw placements;

the swing duration and speed: the swing duration is the duration of the swing phase, while the swing speed is computed from the swing duration and the stride length (Hamers et al, 2006; Hamers et al, 2001).

Muscle tension recording

The animals randomly selected for tension recording (n=4 in both the control and the grafted group) were anaesthetized with ketamine-xylazine at the end of the 3-month survival period and the tibialis anterior and extensor digitorum longus muscles of both the reinnervated and the contralateral control hindlimb were prepared for tension recording. These muscles were chosen for tension recording because the motoneurons innervating them are mainly found in spinal segment L4 (Lowrie et al, 1987). The muscles of the contralateral leg were considered to be suitable controls because their tension increased with age in a similar way to that for the muscles of the normal, unoperated animals. The distal tendons were dissected free and attached to strain gauges, and the exposed parts of the muscles were kept moist with Krebs' saline solution. Isometric contractions were then elicited from the muscles by stimulating the ventral ramus of the L4 spinal nerve with bipolar electrodes. The length of each muscle was adjusted so as to produce the maximum twitch

tension. Single twitch and tetanic (40-100 Hz) contractions were displayed and recorded on a computer; all the additional recording hardware and software were developed by Supertech Ltd (Pécs, Hungary, system "Kellényi"). Maximum tetanic tension was achieved at a stimulation frequency of about 100 Hz. An estimate of the numbers of motor axons supplying the muscles was obtained by stimulating the L4 spinal nerve with stimuli of increasing intensity and recording the stepwise increments of twitch contractions.

Statistical analysis

The non-parametric Mann-Whitney U test and the one-way or two-way ANOVA test with Tukey's all pairwise multiple comparison procedures were used to compare the data on the groups. The tests were used according to the parametric or non-parametric nature of the data. Values are reported throughout the manuscript as means ± S.E.M.

Results

In order to determine whether stem cells that do not produce detectable amounts of neuroprotective molecules *in vitro* are able to adapt to the environment of damaged motoneurons and prevent cell death, neuroectodermal stem cells derived from the telencephalic vesicle wall of E9 p53-deficient mouse embryos were grafted into the lumbar 4 (L4) segment of the spinal cord of rats whose L4 ventral root has been avulsed and subsequently reimplanted (Fig. 1A and see detailed description in Materials and Methods). The clonal stem cell line applied, NE-GFP-4C (ATCC number CRL-2926), was described and characterized in detail earlier (Schlett and Madarász, 1997).

Survival, differentiation and migration of the grafted stem cells

The grafted stem cells ($3x10^5$ stem cells in each case) formed a round mass of green fluorescent protein (GFP)-positive cells in the ventral part of segment L4 and indicated early signs of differentiation by first expressing the embryonic stem cell marker SSEA-1 (stage-specific embryonic antigen-1) at 5 days postoperatively (n=4, Fig. 1B). The cells of the graft later started to differentiate into glial and neuronal cell lines, but at 10 days following grafting (n=4) the graft-derived astrocytes and neurons had not yet migrated away from the grafting site (Fig. 1C). During the next few days, the differentiated cells ceased their GFP expression and largely migrated away from the implantation site, leaving there only limited numbers of differentiated cells (16 days survival, n=4, Fig. 1D). Numerous stem cell-derived neurons (501±84) and astrocytes (465±81) settled throughout segment L4 in the following weeks (1 month survival, n=5, Figs. 1J-1K), while only very few (45±16) oligodendrocytes of graft origin could be detected. The stem cells and their derivatives were rarely seen in contact with the injured motoneurons. Three months after grafting, the astrocytes and neurons were still confined nearly exclusively to the injured L4 segment. By a survival time of 6 months (n=5) their numbers had decreased critically.

Stem cell grafts dramatically improve the reinnervation of hindlimb muscles by the rescued motoneurons

Retrograde labelling from the ventral ramus of the L4 spinal nerve 3 months after grafting revealed that large numbers of axons of surviving motoneurons (up to 65% of the total L4 motoneuron pool) were able to enter the reimplanted root and reinnervate muscles in animals that received a stem cell graft ($3x10^5$ stem cells) at the time of avulsion and reimplantation (ARG animals, Figs. 2A-B). In the non-grafted control animals (AR animals, n=5), however, only minimal numbers of motoneurons (46±5, 4% of the total intact L4 pool) contributed to the reinnervation of the hindlimb muscles (Fig. 2A). Increasing numbers of grafted stem cells ($5x10^4$, 1x, 2x and $3x10^5$ stem cells, n=5 in each group) proved to induce proportionally increasing numbers of surviving motoneurons that reinnervated the targets, suggesting a motoneuron-rescuing mechanism dependent on the numbers of molecules secreted by the grafted cells (Figs. 2A-B). However, the number of grafted cells that could be utilized to rescue the motoneurons and promote regeneration exhibited an optimum. Grafts involving more than $3x10^5$ stem cells (e.g. $5x10^5$ or $1x10^6$ stem cells) caused damage to the host cord, thereby compromising the regenerative effects of the grafted stem cells. Such grafts were therefore excluded from the present study. In the subsequent work reported here each ARG animal received $3x10^5$ stem cells. Morphological reinnervation was confirmed by examinations proving functional reinnervation. The higher numbers of motor units found in the grafted animals (21±1 [ARG] *vs* 4±1 [AR] motor units for the tibialis anterior, and 14±1 [ARG] *vs* 4.5±1 [AR] for the extensor digitorum longus; Figs. 2C-D) produced significantly greater forces in the tibialis anterior (79%±3 operated/intact side [ARG] *vs* 7.5%±2.5 [AR]) and the extensor digitorum longus (73%±3 [ARG] *vs* 13%±4 [AR]) muscles (n=4, Figs. 2E-F). Detailed functional hindlimb movement analysis with the CatWalk system showed that the affected hindlimbs of the ARG animals demonstrated movement pattern features closely approximating to those of intact animals, whereas the AR animals displayed a considerably impaired movement pattern (Fig. 3).

Stem cell graft downregulates glial microenvironment in the host cord

We next investigated the glial environment of the injured motoneurons in the ventral horn of grafted and control animals. Both astroglial and microglial activity are known to moderate cascades of negative effects on damaged neurons of the spinal cord, although the nature of the microglia/macrophages that participate in certain pathological processes is still controversial (Biber et al, 2007; Gaudet et al, 2011). We therefore looked at the glial reactions within the spinal cords of AR and ARG animals in the critical first 10 days after the avulsion injury. At 5 and 10 days after grafting, neuroectodermal stem cell transplantation led to significant decrease in the microglia/macrophage and astroglial reactions throughout segment L4 of ARG animals relative to AR animals (Fig. 4).

Determination of secreted factors expressed in the grafted cord

These data suggested that, in view of the lack of physical contact between the injured and the grafted cells, a paracrine secretory mechanism must be exerted by the graft to decrease the activity of the glial cells of the cord and prevent motoneuron death. To determine the factors acting in the grafted cords, we performed a series of semiquantitative PCR analyses of segment L4 in ARG and AR animals, including neurotrophic and immune factors known to play roles in spinal cord injuries and their experimental treatment (Bartholdi and Schwab, 1997; Ousman and David, 2001). It emerged that on postoperative days 2, 5, 10 and 14 there was no difference between the AR and ARG animals (n=4 in each group) in the mRNA levels of the investigated neurotrophic factors, but the mRNA levels of the interleukins IL-1-alpha, IL-6 and IL-10, tumour necrosis factor-alpha (TNF-alpha) and macrophage inflammatory protein-1-alpha (MIP-1-alpha) were significantly higher in the ARG than in the AR animals, typically at 5 and 10 days following grafting. However, the mRNA production of these factors had declined by 14 days after grafting (Fig. 5).

Differential mRNA expression of cytokines in the stem cells graft and in the ventral horns

To distinguish between graft and host immune factor production, we used the laser microdissection technique to perform a qPCR analysis on identical parts of spinal cord sections (ventral horns) taken from AR and ARG animals and from the stem cell graft (n=5 in each group) The stem cell grafts and the ventral horns of the ARG animals produced considerable amounts of the cytokines investigated, with appreciable increases by 10 days as compared with 5 days after grafting (Figs. 6A-E); IL-10 proved to be an exception, as it was produced in greater amounts by the grafted cells 5 days after grafting. In contrast, the ventral horns of the AR animals produced increased amounts of the mRNAs of these factors at 5 days, with a moderate decline by 10 days after the avulsion injury; IL-10 was again an exception: it was not produced in the control cords at all (Fig. 6C). The cultured NE-GFP-4C cells did not display detectable levels of the mRNAs of any of the factors. At a survival time of 10 days, the ventral horns of the ARG animals exhibited increased mRNA levels of all the factors, including IL-10, relative to the mRNA levels of the AR animals, suggesting a graft-induced upregulation of these factors at the mRNA level in the host cord.

Protein expression patterns of cytokines in the grafted cells and in the spinal cord

To test whether the mRNA levels are translated into protein production, the protein expression patterns of these cytokines were studied by immunohistochemistry. Through the use of mouse-specific antibodies, strong immunoreactivity to all five factors was found to be exerted by the grafted cells at 5 days after grafting (Figs. 6F-J). It was noteworthy that the majority, but not all of the grafted cells were immunopositive for the cytokines tested. However, at 10 days postoperatively only the strong expression patterns of IL-6, TNF-alpha and MIP-1-alpha were maintained. The immunofluorescence of IL-1-alpha and IL-10 was confined to some of the stem cells located at the periphery of the graft. On the other hand, immunohistochemistry with anti-rat/mouse specific antibodies indicated that the ventral horn neurons and glial cells of the ARG animals appeared to produce only IL-6, IL-10 and MIP-1-alpha. The expression patterns were uniform at both 5 and 10 days after grafting. Confocal microscopic analysis of double-labelled

sections revealed that the glial IL-6, IL-10 and MIP-1-alpha reactivity was confined to the astrocytes, and not to the microglia/macrophages of the host cord, even though the degree of astrogliosis in the ARG animals was limited. A similar distribution pattern of these cytokines was observed in the AR animals, but the astroglial density was increased. Despite the relatively high mRNA levels of IL-1-alpha and TNF-alpha, no immunoreactivity to these factors could be detected as compared with the biological positive controls (see Experimental Procedures).

Function-blocking antibodies abolish the neuroprotective effects of the grafted stem cells

To test whether these cytokines are indeed responsible for inducing the prevention of motoneuron death, for 2 weeks we used osmotic pumps to infuse the mixture of function-blocking mouse-specific antibodies produced against all five factors to the grafts (n=5, ARG + 5-factor neutralization). Indeed, retrograde labelling from the ventral ramus of the L4 spinal nerve revealed virtually as few reinnervating motoneurons after 3 months as in the AR animals (57±5 [ARG+5-factor neutralization], 46±5 [AR]; Figs. 7A,D, and E). However, the question remained as to whether the considerable amount of IL-10 (the only cytokine with anti-inflammatory effects in the peripheral immune system) produced by the grafted cells would alone be able to prevent motoneuron death. In a search for an answer to this question, we set up another function-blocking experiment (n=5, ARG + IL-10 neutralization) in which only the anti-IL-10 mouse-specific function-blocking antibody was infused by osmotic pump to the grafted cord. When the IL-10 function was blocked in this way, the reinnervation of denervated hindlimbs was dramatically improved in comparison with that in the AR and ARG + 5-factor neutralization animals (195±10 reinnervating motoneurons, Fig. 7E). In order to test whether isotype-specific immunoglobulins do not have a neutralizing effect on the grafted stem cells, osmotic pumps filled with a mixture of isotype-specific IgGs were used to deliver these IgGs to the site of grafting, and no significant difference relative to the ARG animals was found (n=5, ARG+IgG; 670±72, Fig. 7E). The significant difference in reinnervating motoneuron numbers between the two neutralization groups

reveals a strong modulatory role for the other four factors in the injured cord (Figs. 7E-F); the blocking of IL-10 produced by the grafted cells was only partially able to inhibit the beneficial effect of the graft. To establish whether the major beneficial effect of IL-10 involves the survival and/or the reinnervating capacity of the motoneurons, we made use of anti-choline acetyltransferase (ChAT) immunofluorescence to detect and count the surviving and intact motoneurons, including those "silent motoneurons" that are not able to regenerate their axons into the vacated endoneural sheaths of the reimplanted L4 root. The proportion of surviving motoneurons on the operated side compared to the total intact ChAT $^{+}$ motoneuron pool in segment L4 was dramatically increased in the ARG animals but not in the other experimental groups (Fig. 7G), indicating that IL-10 is mainly responsible for the survival of the motoneurons in this experimental paradigm. On the other hand, the proportion of surviving motoneurons that are able to reinnervate peripheral targets (Fig. 7G) was again improved after blockade of the IL-10 function, which suggests an important, but not overwhelming role for IL-10.

Discussion

We have shown here that, following an avulsion injury grafted embryonic neuroectodermal stem cells successfully prevent motoneuron death by inhibiting microglia/macrophage activity in the injured ventral horn, and thus probably by decreasing the excess glutamate release onto vulnerable motoneurons.

Grafting neuroectodermal stem cells into the spinal cord on one hand induced prominent survival of injured motoneurons and on the other hand the regenerating axons of rescued motoneurons were able to produce functional reinnervation of the denervated hindlimb muscles. However, stem cell-derived neurons were never found to contribute to the reinnervation of reimplanted ventral root. It appeared therefore obvious that the grafted stem cells secreted a number of factors at the site of the lesion in a paracrine fashion that have a direct effect on the survival of the injured motoneuron pool destined to death. It has previously been reported that motoneurons affected by an avulsion

injury of the spinal ventral root containing their axons eventually leads to their death in 10-12 days following injury (Koliatsos et al, 1994; Zhou et al, 2009) and they can be rescued with an anti-excitotoxic treatment provided it starts within 10 days after avulsion (Nogradi et al, 2007).

It remains to be answered, however, to what extent and by what mechanisms the pro-inflammatory cytokines, found to be expressed by the grafted stem cells may contribute to the improved survival and regenerative capacity of injured motoneurons.

It has clearly been shown that IL-10, an anti-inflammatory cytokine in the peripheral immune system has a neuroprotective effect in the CNS, too. IL-10 has been reported to inhibit caspase-3 and NF-κB DNA binding in neurons *in vitro*, thereby preventing the cell death induced by glutamate excitotoxicity (Bachis et al, 2001). Moreover, administration of IL-10 after traumatic or excitotoxic spinal cord injury promoted survival of injured neurons and improved recovery of motor function acting through the IL-10 receptor on the injured neurons, thereby preventing the activation of the apoptotic cascades (Bethea et al, 1999 ; Jackson et al, 2005 ; Zhou et al, 2009). It appears from these *in vitro* and *in vivo* studies that IL-10 possesses a direct neuroprotective effect in the CNS in addition to the well-established anti-inflammatory effects.

The mechanisms of action in the CNS of IL-1-alpha, IL-6 and TNF-alpha, known to be pro-inflammatory cytokines in the peripheral immune system (Commins et al, 2010), are not yet fully understood (Aldskogius, 2011; Glezer et al, 2007; Juttler et al, 2002). In vitro evidence is accumulating that IL-1-alpha, IL-1-beta, IL-6 and TNF-alpha are neuroprotective against excitotoxicity-induced cell death in the CNS via distinct pathways (Carlson et al, 1998, 1999, Liu et al 2011), and that the administration of IL-1-beta, IL-6 and TNF-alpha to the injured murine spinal cord leads to decreases in the levels of microglia/macrophage activation and tissue loss (Klusman and Schwab, 1997). These data strongly support the view that acute or sub-chronic exposure of the highly vulnerable injured motoneuron pool to these pro-inflammatory cytokines is not deleterious, although longer expression patterns of these cytokines may already induce toxic effects. The fact that the grafted stem cells remain clustered at the site of grafting for 10 days and show only limited

differentiation along with a significant rate of cytokine expression levels suggest that this short period of time of stem cell differentiation provides satisfactory neuroprotection for the injured motoneurons along with considerable depression of macrophage and astrocyte activation. It is noteworthy that the stem cell grafts induced expression of some of the cytokines, including IL-10 in the host ventral horn, and this was likely to contribute to their neuroprotective effects. The rapid differentiation process and migration of stem cells appears to cease cytokine expression after this beneficial period of time.

These data, in conjunction with our findings, strongly suggest that pro-inflammatory and anti-inflammatory cytokines selectively secreted by grafted stem cells act in concert to save motoneurons and to promote reinnervation of the target muscles. These results raise the opportunity to investigate whether a local treatment of injured motoneurons with a well-defined set and dose of cytokines may bring about the similarly great extent of cell rescue and reinnervation as treatment with stem cells.

References

Aldskogius H (2011) Mechanisms and consequences of microglial responses to peripheral axotomy. Front. Biosci. Schol. Ed. 3:857-868.

Bachis A, Colangelo AM, Vicini S, Doe PP, De Bernardi MA, Brooker G, Mocchetti, I (2001) Interleukin-10 prevents glutamate-mediated cerebellar granule cell death by blocking caspase-3-like activity. J. Neurosci. 21:3104-3112.

Bartholdi D, Schwab ME (1997) Expression of pro-inflammatory cytokine and chemokine mRNA upon experimental spinal cord injury in mouse: an in situ hybridization study. Eur. J. Neurosci. 9:1422-1438.

Bethea JR, Nagashima H, Acosta MC, Briceno C, Gomez F, Marcillo AE, Loor K, Green J, Dietrich WD (1999) Systemically administered interleukin-10 reduces tumor necrosis factor-alpha production and significantly improves functional recovery following traumatic spinal cord injury in rats. J. Neurotrauma 16:851-863.

Biber K, Neumann H, Inoue K, Boddeke HW (2007) Neuronal 'On' and 'Off' signals control microglia. Trends Neurosci. 30:596-602.

Blits B, Carlstedt TP, Ruitenberg MJ, de Winter F, Hermens WT, Dijkhuizen PA, Claasens JW,

Eggers R, van der Sluis R, Tenenbaum L, Boer GJ, Verhaagen J (2004) Rescue and sprouting of motoneurons following ventral root avulsion and reimplantation combined with intraspinal adeno-associated viral vector-mediated expression of glial cell line-derived neurotrophic factor or brain-derived neurotrophic factor. Exp. Neurol. 189:303-316.

Brown GC, Neher JJ (2010) Inflammatory neurodegeneration and mechanisms of microglial killing of neurons. Mol. Neurobiol. 41:242-247.

Carlson NG, Wieggel WA, Chen J, Bacchi A, Rogers SW, Gahring LC (1999) Inflammatory cytokines IL-1 alpha, IL-1 beta, IL-6, and TNF-alpha impart neuroprotection to an excitotoxin through distinct pathways. J. Immunol. 163:3963-3968.

Commins SP, Borish L, Steinke JW (2010) Immunologic messenger molecules: cytokines, interferons, and chemokines. J. Allergy Clin. Immunol. 125:S53-72.

Demeter K, Herberth B, Duda E, Domonkos A, Jaffredo T, Herman JP, Madarász E (2004) Fate of cloned embryonic neuroectodermal cells implanted into the adult, newborn and embryonic forebrain. Exp. Neurol. *188(2):254-67.*

Eggers R, Hendriks WT, Tannemaat MR, van Heerikhuize JJ, Pool CW, Carlstedt TP, Zaldumbide A, Hoeben RC, Boer GJ, Verhaagen J (2008) Neuroregenerative effects of lentiviral vector-mediated GDNF expression in reimplanted ventral roots. Mol. Cell. Neurosci. 39:105-117.

Gaudet AD, Popovich PG, Ramer MS (2011) Wallerian degeneration: gaining perspective on inflammatory events after peripheral nerve injury. J. Neuroinflammation 8:110.

Giulian D, Vaca K, Corpuz M (1993) Brain glia release factors with opposing actions upon neuronal survival. J. Neurosci. 13:29-37.

Glezer I, Simard AR, Rivest S (2007) Neuroprotective role of the innate immune system by microglia. Neuroscience 147:867-883.

Hahn JS, Aizenman E, Lipton SA (1988) Central mammalian neurons normally resistant to glutamate toxicity are made sensitive by elevated extracellular Ca2+: toxicity is blocked by the N-methyl-D-aspartate antagonist MK-801. Proc. Natl. Acad. Sci. U S A 85:6556-6560.

Hamers FP, Koopmans GC, Joosten EA (2006) CatWalk-assisted gait analysis in the assessment of spinal cord injury. J. Neurotrauma 23:537-548.

Hamers FP, Lankhorst AJ, van Laar TJ, Veldhuis WB, Gispen WH (2001) Automated quantitative gait analysis during overground locomotion in the rat: its application to spinal cord contusion and transection injuries. J. Neurotrauma 18:187-201.

Hell RC, Costa MM, Goes AM, Oliveira AL (2009) Local injection of BDNF producing mesenchymal stem cells increases neuronal survival and synaptic stability following ventral root avulsion. Neurobiol. Dis. 33:290-300.

Jackson CA, Messinger J, Peduzzi JD, Ansardi DC, Morrow CD (2005) Enhanced functional recovery from spinal cord injury following intrathecal or intramuscular administration of poliovirus replicons encoding IL-10. Virology 336:173-183.

Jais A, Klein D, Wolfesberger B, Walter I (2011) Gene expression profile of vascular endothelial

growth factor (VEGF) and its receptors in various cell types of the canine lymph node using laser capture microdissection (LCM). Vet. Immunol. Immunopathol. 140:207-214.

Juttler E, Tarabin V, Schwaninger M (2002) Interleukin-6 (IL-6): a possible neuromodulator induced by neuronal activity. Neuroscientist 8:268-275.

Klein D (2002) Quantification using real-time PCR technology: applications and limitations. Trends Mol. Med. 8:257-260.

Klusman I, Schwab ME (1997) Effects of pro-inflammatory cytokines in experimental spinal cord injury. Brain Res. 762:173-184.

Koliatsos VE, Price WL, Pardo CA, Price DL (1994) Ventral root avulsion: an experimental model of death of adult motor neurons. J. Comp. Neurol. 342:35-44.

Lowrie MB, Krishnan S, Vrbova G (1987) Permanent changes in muscle and motoneurones induced by nerve injury during a critical period of development of the rat. Brain Res. 428:91-101.

McNaught KS, Brown GC (1998) Nitric oxide causes glutamate release from brain synaptosomes. J. Neurochem. 70:1541-1546.

Nogradi A, Szabo A, Pinter S, Vrbova (2007) Delayed riluzole treatment is able to rescue injured rat spinal motoneurons. Neuroscience 144:431-438.

Nogradi A, Vrbova G (1996) Improved motor function of denervated rat hindlimb muscles induced by embryonic spinal cord grafts. Eur. J. Neurosci. 8:2198-2203.

Nogradi A, Vrbova G (2001) The effect of riluzole treatment in rats on the survival of injured adult and grafted embryonic motoneurons. Eur. J. Neurosci. 13:113-118.

Ousman SS, David S (2001) MIP-1alpha, MCP-1, GM-CSF, and TNF-alpha control the immune cell response that mediates rapid phagocytosis of myelin from the adult mouse spinal cord. J. Neurosci. 21:4649-4656.

Penas C, Casas C, Robert I, Fores J, Navarro X (2009) Cytoskeletal and activity-related changes in spinal motoneurons after root avulsion. J. Neurotrauma 26:763-779.

Pinter S, Gloviczki B, Szabo A, Marton G, Nogradi A (2010) Increased survival and reinnervation of cervical motoneurons by riluzole after avulsion of the C7 ventral root. Neurotrauma 27:2273-2282.

Regan RF, Choi DW (1991) Glutamate neurotoxicity in spinal cord cell culture. Neuroscience 43:585-591.

Schlett K, Madarasz E (1997) Retinoic acid induced neural differentiation in a neuroectodermal cell line immortalized by p53 deficiency. J. Neurosci. Res. 47:405-415.

Su H, Zhang W, Guo J, Guo A, Yuan Q, Wu W (2009) Neural progenitor cells enhance the survival and axonal regeneration of injured motoneurons after transplantation into the avulsed ventral horn of adult rats. J. Neurotrauma 26:67-80.

Tikka TM, Koistinaho JE (2001) Minocycline provides neuroprotection against

N-methyl-D-aspartate neurotoxicity by inhibiting microglia. J. Immunol. 166:7527-7533.

Zádori A, Agoston VA, Demeter K, Hádinger N, Várady L, Köhídi T, Göbl A, Nagy Z, Madarász E (2011) Survival and differentiation of neuroectodermal cells with stem cell properties at different oxygen levels. Exp. Neurol. 227(1):136-48.

Zhou Z Peng X, Insolera R, Fink DJ, Mata M (2009) IL-10 promotes neuronal survival following spinal cord injury. Exp. Neurol. 220:183-190.

Figures and figure legends:

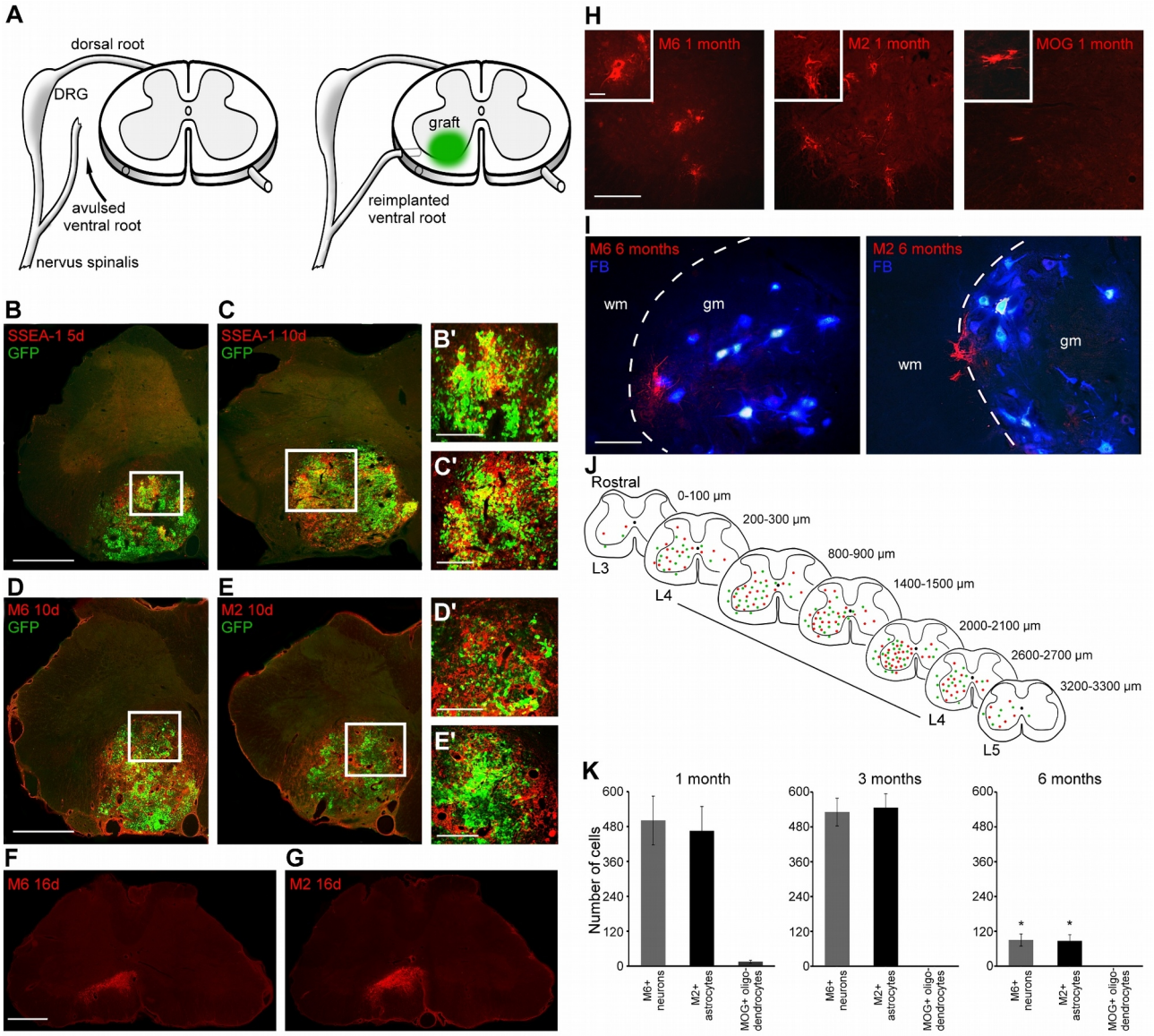

Figure 1.

Differentiation and migration of grafted stem cells and their derivatives in the spinal cord.

A. Schematic drawing showing the surgical procedure of avulsion, stem cell grafting and reimplantation of the avulsed L4 ventral root. **B,C.** Expression of embryonic stem cell marker SSEA-1 by the grafted stem cells 5 and 10 days after transplantation. **D,E.** Initial differentiation of the grafted stem cells to M6+ neurons and M2+ astrocytes, accompanied by the loss of GFP expression. **F,G.** Dispersion of the differentiated stem cells from the site of grafting, where only limited numbers of astrocytes and neurons of graft origin remain. **H.** Numerous M6+ neurons and

M2+ astrocytes are present in the cord 1 month after grafting, whereas MOG+ oligodendrocytes are rarely found. **I.** Only a few stem cell-derived neurons and astrocytes, but no oligodendrocytes are located in the host cord 6 months following transplantation. **J.** Distribution of M2+ astrocytes (green dots) and M6+ neurons (red dots) in the injured L4 segment one month following grafting in a representative ARG animal. Each spinal cord cross-section represents a 100 µm thick segment of the cord. The vast majority of the stem cell-derived cells are located in the affected L4 segment. **K.** The absolute numbers of stem cell-derived neurons, astrocytes and oligodendrocytes are shown at various time points after grafting, n=5. Data are presented as mean +/- S.E.M, $p<0.05$. The one-way ANOVA analysis with Tukey's post-hoc tests was performed. Scale bar in **B-G**= 500 µm, **B'-E'**= 200 µm, **H**= 200 µm and 50 µm (insets), **I**= 100 µm

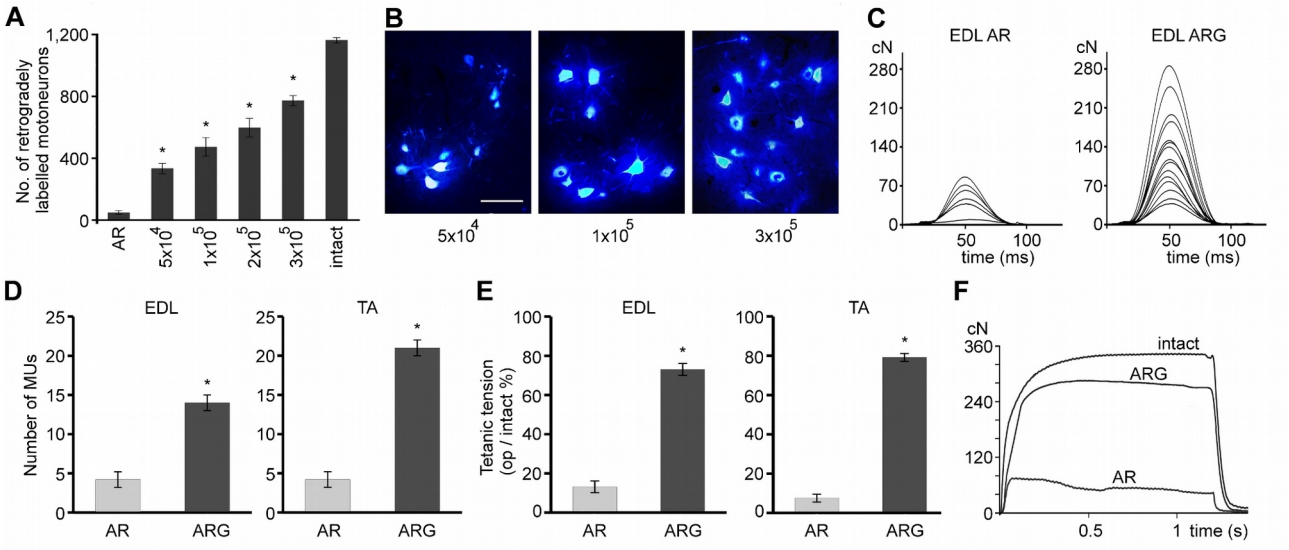

Figure 2.

Reinnervation of peripheral targets by injured motoneurons rescued by grafted stem cells.

A,B. The extent of reinnervation of peripheral targets depends on the number of grafted stem cells. In control animals (AR), only 46±5 retrogradely labelled cells were found, while the transplantion of $3x10^5$ stem cells resulted in 736±32 reinnervating motoneurons, n=5. **C,D.** The extensor digitorum longus (EDL) and the tibialis anterior (TA) muscles of grafted (ARG) rats are innervated

by significantly greater numbers of motor axons than are the muscles of AR animals; individual twitch contractions of motor units (MU) are shown in **C**, n=4. **E,F.** Greater numbers of reinnervating motor axons produced greater maximum tetanic muscle contractions in ARG animals, n=4; individual tetanic curves are shown in **F.** Data are presented as mean +/- S.E.M, $p<0.05$. Data were analysed by applying the non-parametric Mann-Whitney U test or one-way ANOVA analysis with Tukey's post-hoc tests was used. Scale bar in **B**= 100 μm.

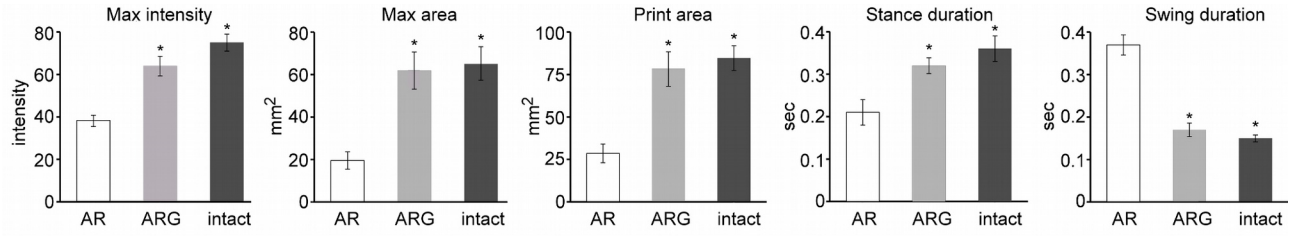

Figure 3.

Results of CatWalk automated gait analysis system.

Various of the gait analysis parameters displayed significant differences between the AR (n=5) and ARG animals (n=5), but not between the ARG and intact animals (n=5), reflecting a nearly complete restoration of the hindlimb function in the grafted animals 3 months after transplantation. Error bars, S.E.M, $p<0.05$. *= significant difference relative to AR animals. The one-way ANOVA analysis with Tukey's post-hoc test was used.

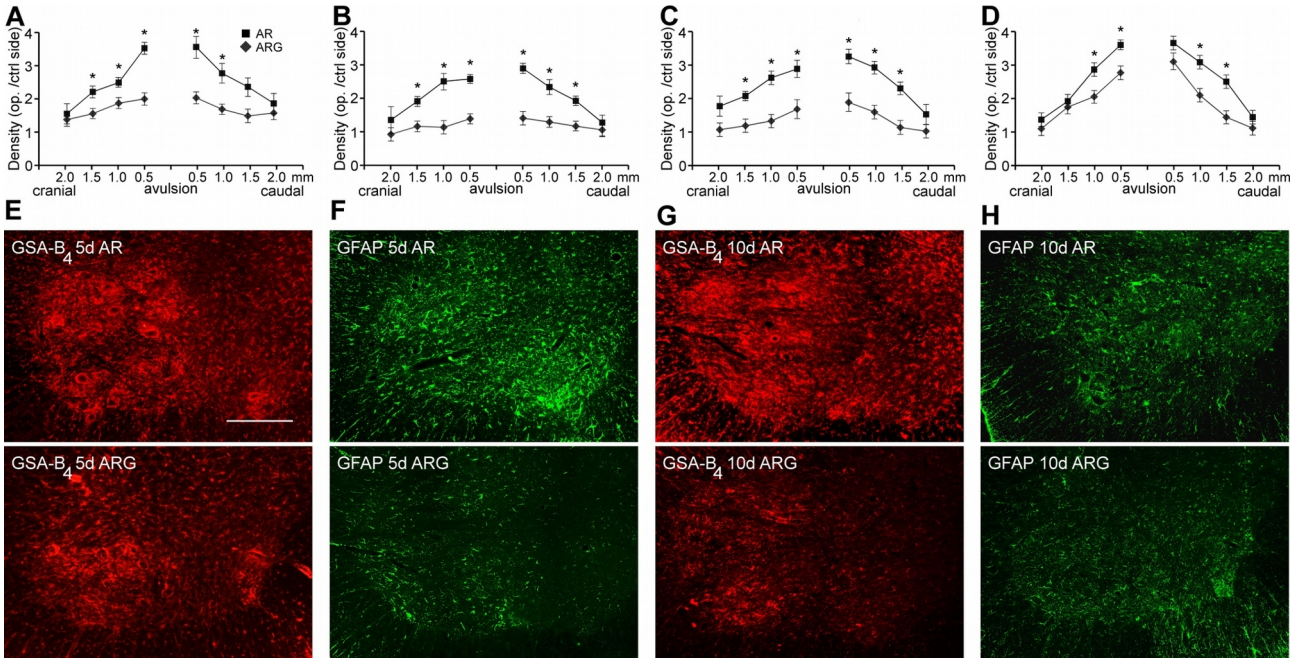

Figure 4.

Astrocytic and microglial/macrophage reactions in grafted and control spinal cords.

A,B. Reduced astroglial (GFAP) and microglial (GSA B $_4$ isolectin) densities are shown in spinal segment L4 of ARG animals. Asterisks indicate the significant differences in density between AR and ARG animals at various distances from the site of avulsion, n=5. Data are presented as mean +/- S.E.M, $p<0.05$. The two-way ANOVA analysis with Tukey's post-hoc tests was used. Scale bar in **B**= 250 µm.

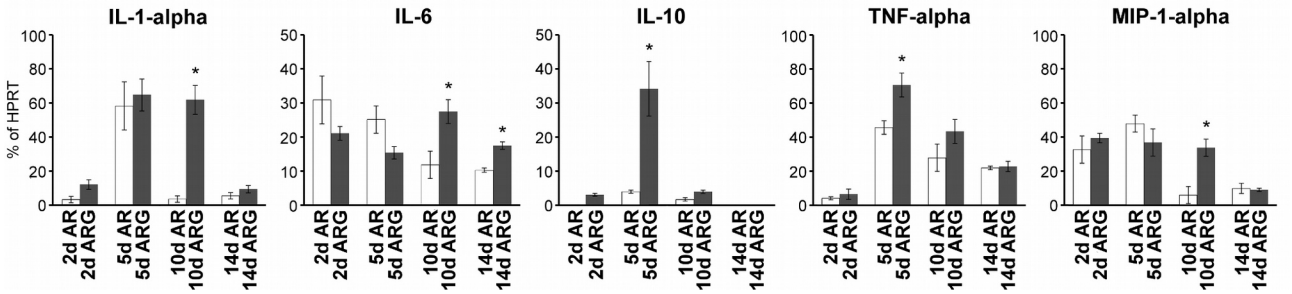

Figure 5.

Results of semiquantitative PCR studies on the production of cytokines

Semiquantitative PCR analysis of cytokine mRNA levels in the injured (AR) or grafted (ARG) L4 segment. Only those factors are shown that displayed a significant difference at any timepoint. Note the great amount of IL-10 mRNA produced in the grafted L4 segment of the ARG animals

(n=4 in each group). *=significant difference between the ARG and AR animals at the same timepoint. The non-parametric Mann-Whitney U test was used.

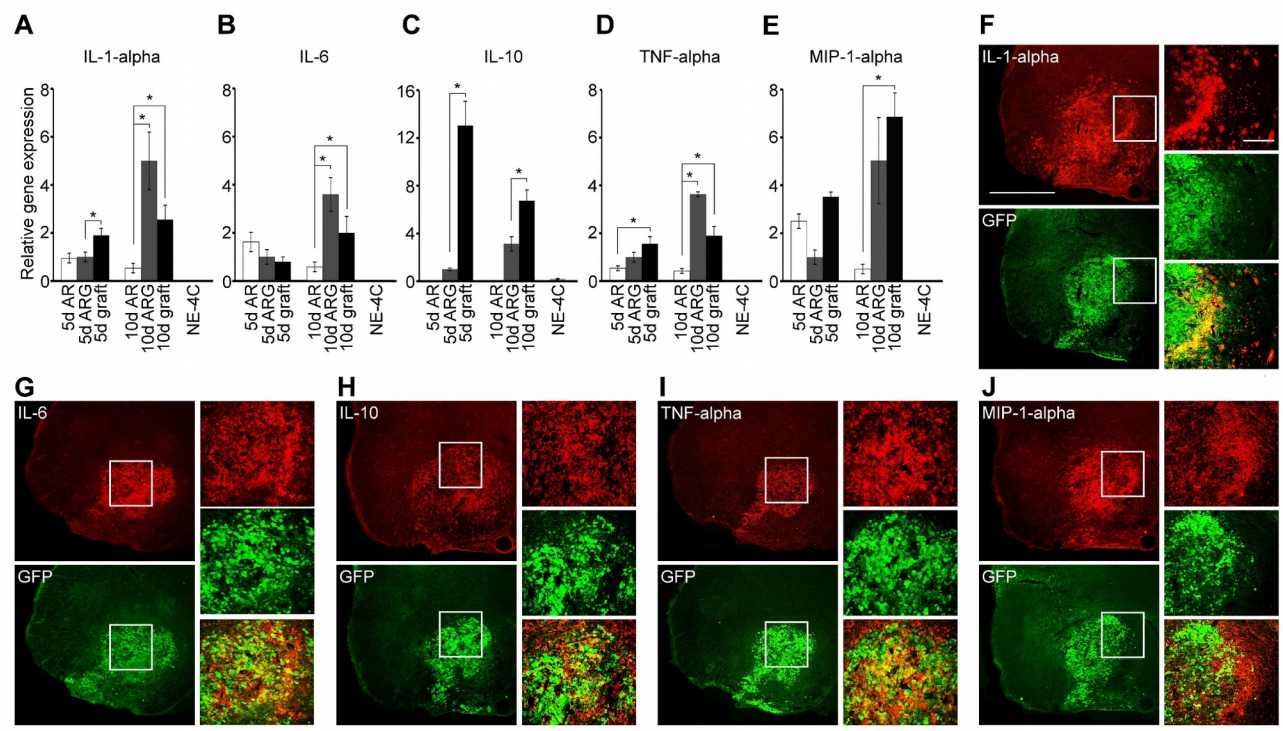

Figure 6.

Elevated mRNA levels and immunohistochemical detection of cytokines produced by the grafted stem cells

A-E. Relative gene expression levels of various cytokines in the ventral horns of AR and ARG animals and in the grafts removed by laser microdissection. There were significant increases in the RNA levels of all factors, and of IL-10 in the ventral horns and in the grafts of ARG animals by 10 days after grafting relative to the data at 5 days, n=4. IL-10 was produced only in the grafted cords, mainly by the grafted cells at 5 days after transplantation. Ventral horns of 5d ARG animals are taken as 1 unit. RNA levels of intact ventral horns are not shown as they were negligible. **F-J.** Immunohistochemical detection of the murine factors produced by the grafted cells at 5 days after transplantation. Note the partial expression pattern shown by the grafted cells, especially in the case of MIP-1-alpha, partially due to declining GFP activity. Data are presented as mean +/- S.E.M,

p<0.05. The one-way ANOVA analysis with Tukey's post-hoc test was used. Scale bar in **B**= 500 µm and 50 µm in insets.

Figure 7.

Function-blocking antibodies inhibit the effects of stem cell grafts on motoneuron survival and regeneration

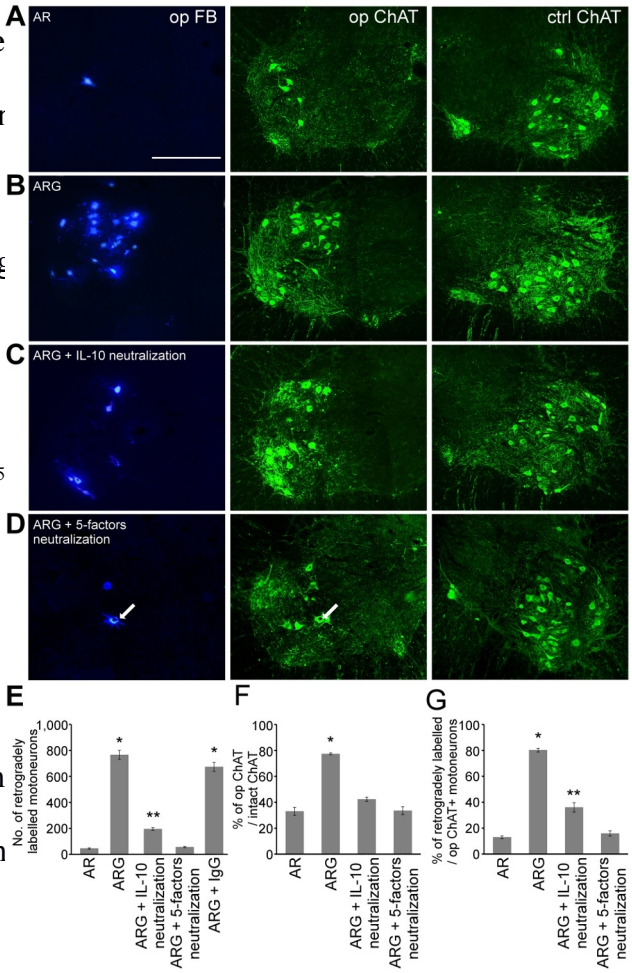

A. Retrogradely labelled (FB^+) and surviving ($ChAT^+$) motoneurons in AR animals. Note the very few reinnervating motoneurons. **B.** Results of retrograde labelling in ARG animals ($3x10^5$ stem cells). Nearly all surviving ($ChAT^+$) cells seem to be able to reinnervate the ventral root. **C,D.** Limited numbers of reinnervating cells can be seen in ARG animals treated with function-blocking antibodies, especially in the case of neutralization against all 5 factors. Diagram showing the numbers of retrogradely labelled neurons in various experimental paradigms. Neutralization treatment against all 5 factors resulted in as low numbers of retrogradely labelled neurons as in AR animals, while treatment with isotype-specific IgGs (ARG+IgG) did not yield significantly less motoneuron survival compared with ARG animals, n=5. **F.** The percentage of surviving injured motoneurons is shown by the proportion of $ChAT^+$ operated/intact motoneurons in animals with various experimental paradigms. As neutralization of IL-10 considerably reduces the number of surviving motoneurons, IL-10 appears to be a strong survival factor for injured motoneurons, n=5. **G.** Percentages of reinnervating

(FB^+) motoneurons in various groups (FB^+/op. $ChAT^+$ motoneurons). Note the reinnervating ability of motoneurons in ARG animals and the moderate ability after neutralization with IL-10 antibody, n=5. *=significant difference between ARG and AR, ARG+IL-10 neutralization and ARG+5-factor neutralization groups (SEM, $p<0.05$). **=significant difference between ARG+IL-10 neutralization and ARG+5-factor neutralization groups (S.E.M, $p<0.05$). The one-way ANOVA analysis with Tukey's post-hoc test was performed. Scale bar in **A-D**= 250 μm. Data are presented as mean +/- S.E.M.